

# A Method for the Measurement of Site-Specific Tautomeric and Zwitterionic Microspecies Equilibrium Constants

Joseph C. D'Angelo and Timothy W. Collette\*

National Exposure Research Laboratory, U.S. Environmental Protection Agency, 960 College Station Road, Athens, Georgia 30605

**We describe a method for the individual measurement of simultaneously occurring, unimolecular, site-specific “microequilibrium” constants as in, for example, prototropic tautomerism and zwitterionic equilibria. Our method represents an elaboration of that of Nygren et al. (*Anal. Chem.* 1996, 68, 1706–10), which thereby becomes generalized and improves the accuracy. Specifically, by making spectral measurements as a function of temperature, we demonstrate the ability to determine site-specific microenthalpies unambiguously. Analysis proceeds via multivariate nonlinear regression modeling of, for example, the Gibbs–Helmholtz relation. Additional determinations of macroscopic equilibrium constants as a function of temperature, in combination with the previously determined microenthalpies, in turn enables the determination of all remaining site-specific thermodynamic parameters, i.e., microentropies, micro free energies, and/or microequilibrium constants, and moreover allows us to resolve and measure the spectra of tautomeric isocoulomers. To our knowledge, we have hereby devised the first such universally applicable and accurate measurement method on record.**

Current process models for predicting the dispersal of organic compounds released to the environment are based on the assumption that these compounds exist exclusively as neutral species with simple covalent attachments.<sup>2</sup> Due to the chemical complexity of many compounds of industrial importance, e.g., pesticides, dyes, etc., this assumption is untenable under a wide variety of environmental circumstances. Indeed, failure to consider speciation may constitute the largest source of uncertainty in organic chemical exposure assessment because the processes that determine chemical transport and transformation are greatly altered when neutral chemicals ionize, tautomerize, or form chemical complexes. Hence, to reduce this source of uncertainty, we have set out to develop and apply analytical methodology that will allow us to identify and quantify individual species of complex chemicals in, for example, water as a function of pH. The work reported herein provides the mathematical and methodological framework for an accurate and generally applicable solution to this problem.

The  $pK_a$  is of particular relevance to environmental process modeling since it describes the degree of ionization of a compound: a property that greatly affects its aqueous solubility<sup>3</sup> and largely determines its propensity to sorb to soil and sediment.<sup>2</sup> While measurement of  $pK_a$  for ordinary amphiprotic compounds is straightforward, the situation with regard to those compounds that may simultaneously ionize to form an internal, i.e., zwitterionic, salt is significantly more problematic. Specifically, there has been a longstanding need for an unequivocally accurate and general method for the experimental determination of tautomeric and zwitterionic microspecies equilibrium constants, the lack of which has precluded the acquisition of relevant data upon which to conceptualize predictive models for this phenomenon and then to evaluate their performance. EPA's SPARC (SPARC Performs Automatic Reasoning in Chemistry) physicochemical properties algorithm<sup>4</sup> has been developed to (predictively) calculate, inter alia, the ionization  $pK_a$ 's for organic compounds<sup>5–7</sup> using fundamental chemical structure theory. SPARC has undergone extensive validity testing with unitary deprotonations;<sup>5–7</sup> consequently, ongoing development of SPARC with regard to prototropic tautomerism will be closely coupled to application of this experimental method.

The specific equilibria with which, for the purpose of demonstrating our method, we concern ourselves here (Figure 1), are representative of zwitterion formation in general.<sup>8,9</sup> The two ionizable sites of 3-hydroxypyridine (CAS No.: 109-00-2), viz., the aromatic hydroxyl and the pyridinium cation, have long been recognized to deprotonate with an appreciable degree of simultaneity.<sup>10</sup> The two cationic site-specific or “microscopic” dissociation reactions,  $k_1$  and  $k_2$  (site designation numbers are arbitrary), combine to produce the aggregate or “macroscopic” cationic deprotonation reaction,  $K_1$ . Similarly, the two electrically neutral “isocoulomers”, viz., the dipolar zwitterion and the tautomericly coupled neutral species, each separately deprotonate, with equilibrium constants designated (according to a numerical sequence

(1) Nygren, J.; Andrade, J. M.; Kubista, M. *Anal. Chem.* 1996, 68, 1706–10.  
(2) Kollig, H. P., Ed. *Environmental Fate Constants for Organic Chemicals Under Consideration for EPA's Hazardous Waste Identification Projects*, U.S.E.P.A., Athens, GA, Pub. No. EPA/600/R-93/132, and references cited therein, 1993.

(3) Albert, A.; Serjeant, E. P. *Ionization Constants of Acids and Bases*, Butler & Tanner Ltd.: Frome and London, 1962, Chapter 6, pp 106–12.  
(4) Karickhoff, S. W.; McDaniel, V. K.; Melton, C. M.; Vellino, A. N.; Note, D. E.; Carreira, L. A. *Environ. Toxicol. Chem.* 1991, 10, 1405–16.  
(5) Hilal, S. H.; Carreira, L. A.; Melton, C. M.; Baughman, G. L.; Karickhoff, S. W. *J. Phys. Org. Chem.*, 1994, 7, 122–41.  
(6) Hilal, S. H.; Karickhoff, S. W.; Carreira, L. A. *Quant. Struct. Act. Relat.* 1995, 14, 348–55.  
(7) Hilal, S. H.; Elshabrawy Y.; Carreira, L. A.; Karickhoff, S. W.; Toubar, S. S.; Rizk, M. *Talanta* 1996, 43, 607–19.  
(8) Adams, E. Q. *J. Am. Chem. Soc.* 1916, 38, 1503–10.  
(9) Edsall, J. T.; Blanchard, M. H. *J. Am. Chem. Soc.* 1993, 55, 2337–53.  
(10) Albert, A.; Phillips, J. N. *J. Chem. Soc.* 1956, 1294–303.

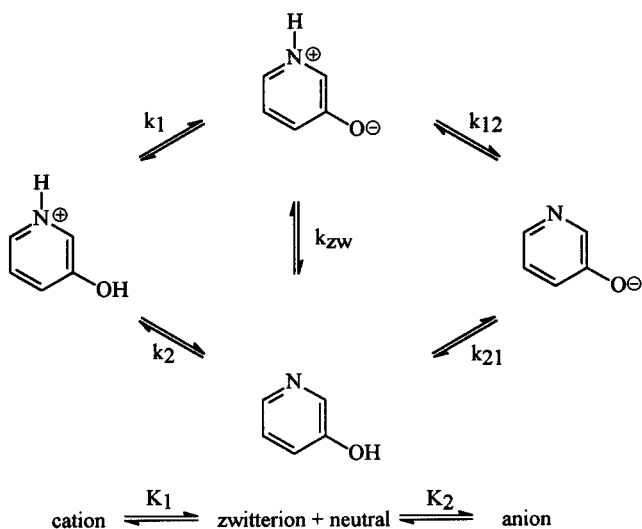


Figure 1. Reaction schematic of situation-specific zwitterionic microreaction equilibria for 3-hydroxypyridine. We arbitrarily enumerate the hydroxyl as site one and the pyridinium as site two. The microequilibrium constant subscripts correspond to the enumerated deprotonation sites, and the order of the subscripts from left to right corresponds to the sequence in which the sites have, with increasing pH, deprotonated. Hence, the last subscript on the right indicates the particular site undergoing deprotonation for the given microequilibrium constant. The quantitative aggregate of the two cationic (or anionic) microequilibria combine to produce the titrimetrically observed macroequilibrium constants  $K_1$  and  $K_2$ .

scheme by Hill<sup>11</sup>) as  $k_{12}$  and  $k_{21}$ , respectively, and also combine to produce an aggregate macroscopic (anionic) deprotonation reaction,  $K_2$ . The relationships among the various equilibrium constants are as follows (cf. Edsall and Blanchard<sup>9</sup> and references cited therein):

$$K_1 = k_1 + k_2 \quad (1)$$

$$\frac{1}{K_2} = \frac{1}{k_{12}} + \frac{1}{k_{21}} \quad (2)$$

$$K_1 K_2 = k_1 k_{12} = k_2 k_{21} \quad (3)$$

And since the site-specific deprotonations are tautomericly coupled, the zwitterionic ratio is given by

$$k_1/k_2 = k_{zw} = k_{21}/k_{12} \quad (4)$$

Given that there are three independent equations, eqs 1–3, in the four unknowns  $k_1$ ,  $k_2$ ,  $k_{12}$ , and  $k_{21}$ , knowledge of any one of the four microconstants is sufficient to specify the other three.<sup>9</sup> It is unfortunately the case that previously devised methods of microconstant measurement are usually predicated upon assumptions, *vide supra*, which render them insufficiently accurate for subjection to theoretical modeling. Hence, our experimental measurements will buttress the accuracy of algorithms, e.g., SPARC, developed for predicting the necessarily refined distinctions between zwitterionic deprotonations and associated tautomeric equilibria.

Aside from its value to environmental modeling, the zwitterion ratio is a more generally important physicochemical parameter.

For example, accurate assessment of this parameter should be useful in biochemistry for elucidating the energetics of both protein folding and enzyme–substrate interactions.<sup>12</sup> A specific instance in which accurate computation of charge speciation is important for analytical chemistry applications is in the estimation of mobilities in capillary zone electrophoresis,<sup>13</sup> where such estimates are utilized for the selection of initial experimental conditions. In addition, the methodology presented herein should prove useful to thermodynamicists, in that all the important parameters for describing equilibria ( $k$ ,  $\Delta H$ ,  $\Delta G$ ,  $\Delta S$ ) can now be obtained with site specificity for very complex, polyfunctional molecules.

There have been a limited number of reports of zwitterionic equilibrium studies (cf. Hilal<sup>6</sup> and references cited therein). However, these initial investigations all relied upon reasonable and plausible ad hoc assumptions, which admittedly subjected the results to systematic error. Wegschieder (cf. Edsall and Blanchard<sup>9</sup> and references cited therein) was perhaps the first to suggest the efficacy of estimating microconstant values for particular site-specific reactions by measuring the macroconstant for a chemically analogous reaction. Specifically, he suggested that the deprotonation of an amino group in a given amino ester could be used to estimate the corresponding microscopic deprotonation in the corresponding amino acid. Subsequently, Benesch and Benesch<sup>14</sup> were among the first to use a spectroscopic method, wherein it is assumed that the extinction coefficient maximum for absorption of a given moiety, e.g., the cysteine S<sup>−</sup> group in the (ultraviolet) region between 2300 and 2400 Å, is immutable to deprotonation of a tautomericly coupled site, e.g., the phenol moiety. Given the shift in the frequency of said maximum with change in pH, Benesch and Benesch were well aware of the limitations of this technique. Yet later, Wrathall, et al.<sup>15</sup> described a calorimetric method based on the assumption that the enthalpy change of chemical analogues was retained by the corresponding moieties of the compound (again cysteine) under study.

To date, what are possibly the only direct determinations of zwitterionic microconstants have been those obtained via NMR.<sup>16–18</sup> With the NMR technique, the relevant parameter for determining the degree of ionization is the chemical shift  $\delta$ . As stated by Rabenstein,<sup>16</sup> when exchange of the acidic proton between the occupied and deprotonated forms is rapid on the NMR time scale, the chemical shifts of the exchange-averaged resonances provide a measure of the fractional ionization.<sup>19</sup> As elucidated by Shrager et al.,<sup>18</sup> the observed chemical shift,  $\delta_A$ , of a particular site, A, is the concentration weighted average of the chemical shift parameters at site A for tautomericly coupled microspecies.

As is the case for other isothermal spectroscopic techniques, there is, in general, an insufficiency of information in NMR spectra to unambiguously determine all of the necessary tautomericly

(12) Jaenicke, R., Ed. *Protein Folding*; Elsevier: Amsterdam, 1980.

(13) Weinberger, R. *Practical Capillary Electrophoresis*; Academic Press, Inc.: New York, 1993; Chapters 2 and 3, pp 17–80.

(14) Benesch, R. E.; Benesch, R. *J. Am. Chem. Soc.*, **1955**, *77*, 5877–81.

(15) Wrathall, D. P.; Izatt, R. M.; Christensen, J. J. *J. Am. Chem. Soc.* **1964**, *86*, 4779–83.

(16) Rabenstein, D. L. *J. Am. Chem. Soc.* **1973**, *95*, 2797–803.

(17) Griffith, R., Jr.; Pillai, L.; Greenberg, M. S. *J. Solution Chem.*, **1979**, *8*, 601–13.

(18) Shrager, R. I.; Cohen, J. S.; Heller, S. R.; Sachs, D. H.; Schechter, A. N. *Biochemistry*, **1972**, *11*, 541–7.

(19) Grunwald, E.; Loewenstein, A.; Meiboom, S. *J. Chem. Phys.* **1957**, *27*, 641–2.

(11) Hill, T. L. *J. Phys. Chem.* **1944**, *48*, 101–11.

coupled parameters.<sup>18</sup> Nevertheless, there may be specific cases<sup>16–18</sup> where one ionization site is sufficiently removed in distance such that the protonation state of that site does not affect the chemical shift of the site A used for analysis. In such cases, the microspecies concentrations can be determined uniquely.<sup>16,17</sup> This situation is analogous to the assumption of absorbance immutability of Benesch and Benesch<sup>14</sup> but possibly with, in such cases, significantly greater accuracy.

We will show herein that the key to accurate determination of microconstants is to introduce further dimensionality into the experiment. Although isocoulomers exist in direct proportion to each other, and are thus linearly dependent upon each other, throughout an entire span of pH, their relative proportions change with temperature according to, for example, the Gibbs–Helmholtz relation. In fact, temperature variation<sup>20</sup> (and other more recent methods of extending dimensionality<sup>21</sup>) has long been employed in the the similar problem of estimating conformer populations in solution. Thus, where titrimetry alone is inadequate, one may similarly produce the requisite resolution of tautomers by extending isothermal global spectroscopic analysis of pH-dependent acid/base equilibria<sup>22</sup> into the temperature domain. Such a procedure is, however, predicated upon sufficient temperature invariance of the relevant species' spectra, and this prerequisite may not hold in all cases.<sup>23</sup> Recently, Nygren et al.<sup>1</sup> applied the van't Hoff relation, a linearized transformation of Gibbs–Helmholtz, to characterize monomer/dimer equilibria using temperature variations. Their method, however, was dependent on acquiring the isolated monomer spectra of their compounds by using appropriately limiting dilute solutions. Neither chemical nor physical methods are, in and of themselves, capable of resolving the spectra of isocoulomers and therefore of obtaining microconstants, because, *vide supra*, it is impossible to know with assurance a priori when or if species isolation has in fact occurred.

#### MATHEMATICAL DESCRIPTION

Given Beer's law,  $A = \epsilon bc$ , it is important for our purposes here to recall that the molar absorptivity (extinction coefficient),  $\epsilon$ , is a characteristic constant of the material proportional to the absorbing cross-sectional area of the molecule<sup>24</sup> and is therefore largely, although not completely, independent of temperature.<sup>23</sup> We thus, with no loss of generality, incorporate the cell's path length,  $b$ , into the absorptivity coefficient,  $e = \epsilon b$ . For the four absorbing species represented by Figure 1, we then have for the absorbance,  $A$  at any particular pH,  $\tau$ , and wavelength,  $\lambda$ .

$$A_{\lambda\tau} = e_{\lambda 1}c_{1\tau} + e_{\lambda 2}c_{2\tau} + e_{\lambda 3}c_{3\tau} + e_{\lambda 4}c_{4\tau} \quad (5)$$

In matrix terms, for the general case of  $w$  wavelengths,  $s$  number of species, and  $p$  number of pH measurements, we have

$$\mathbf{A}_{wp} = \mathbf{E}_{ws}\mathbf{C}_{sp} \quad (6)$$

where  $\mathbf{A}$  is a matrix consisting of  $p$  columns of absorbance spectra

(20) Abraham, R. J.; Bretschneider, E. In *Internal Rotation in Molecules*; Orville-Thomas, W. F., Ed.; Wiley-Interscience: New York, 1974; Chapter 13, pp 481–584.

(21) Saltiel, J.; Sears, D. F., Jr.; Choi, J.-O.; Sun, Y.-P.; Eaker, D. W. *J. Phys. Chem.* **1994**, *98*, 35–46.

(22) Frans, S. D.; Harris, J. M. *Anal. Chem.* **1984**, *56*, 466–70.

(23) Saltiel, J.; Choi, J.-O.; Sears, D. F., Jr.; Eaker, D. W.; Mallory, F. B.; Mallory, C. W. *J. Phys. Chem.* **1994**, *98*, 13162–70, and references cited therein.

(24) Hughes, H. K.; et al. *Anal. Chem.* **1952**, *24*, 1349–54.

at each of the various pH's, and where the spectra are sampled at  $w$  discrete frequencies;  $\mathbf{E}$  is a matrix consisting of columns of molar absorptivity coefficient spectra for each of the  $s$  microspecies at the same discrete frequencies  $w$  as in  $\mathbf{A}$ , and  $\mathbf{C}$  is a matrix consisting of  $p$  columns of microspecies concentrations at each of the sampled pH's, with each row representing a different microspecies concentration profile. For our example in this scheme, species 1 represents the cation, species 2 represents the zwitterion, species 3 represents the neutral molecule, and species 4 represents the anion. The concentrations of the cation and anion both vary with pH in a manner typical of any diprotic acid. The concentration of the isocoulomers is given as

$$C_{2\tau} = c_a \frac{k_1 H_\tau}{D(H_\tau)} \quad (7)$$

for the zwitterion and

$$C_{3\tau} = c_a \frac{k_2 H_\tau}{D(H_\tau)} \quad (8)$$

for the neutral, where  $c_a$  is the analytical concentration of 3-hydroxypyridine, and where

$$D(H_\tau) = H_\tau^2 + K_1 H_\tau + K_1 K_2 \quad (9)$$

It is of particular importance to note that the isocoulomers exist in direct proportion to each other throughout the entire pH range. They are therefore mathematically linearly dependent upon one another, and there is, in general, no isothermal experiment, e.g., titration, spectroscopic, etc., that can determine the concentration of either species uniquely. In fact, the number of possible hypothetical microconstant solution pairs consistent with any temperature-invariant titration experiment is in fact infinite.

We wish therefore to obtain a direct and unequivocally accurate measurement of microconstants and their associated zwitterionic equilibria. This may be accomplished by employing the Gibbs–Helmholtz relation, which provides an experimental relation for the variance of an equilibrium constant as a function of temperature, *viz.*,

$$k_{aT} = k_{a0} \exp\left[\frac{\Delta H_a}{R}\left(\frac{1}{T_0} - \frac{1}{T}\right)\right] \quad (10)$$

where  $\Delta H_a$  is the “microenthalpy” specific to the deprotonation sequence a,  $T$  is an arbitrary absolute temperature,  $k_{a0}$  is the equilibrium microconstant for the deprotonation sequence a at the defined absolute base temperature,  $T_0$ , and  $k_{aT}$  is the microconstant for the deprotonation sequence a at temperature  $T$ . This particular form assumes only that the temperature variation is limited enough for the microenthalpy to be considered effectively constant. Since at any temperature,  $K_{1T} = k_{1T} + k_{2T}$ , we have for the temperature dependence of the macroconstant

$$K_{1T} = k_{10} \exp\left[\frac{\Delta H_1}{R}\left(\frac{1}{T_0} - \frac{1}{T}\right)\right] + k_{20} \exp\left[\frac{\Delta H_2}{R}\left(\frac{1}{T_0} - \frac{1}{T}\right)\right] \quad (11)$$

where  $k_{10}$  and  $k_{20}$  are used to indicate the microconstants ( $k_1$  and  $k_2$ ) extant at the defined base temperature.

To demonstrate this contention, and in order to simplify the coming discussion, we define the “reduced” microenthalpy,  $h_i = \Delta H_i/R$ , for  $i = 1, 2$ , and also define

$$t = \left( \frac{1}{T_0} - \frac{1}{T} \right) \quad (12)$$

or equivalently,

$$t = \frac{1}{T_0} \left( 1 - \frac{T_0}{T} \right) \quad (13)$$

Note that  $t$  is a monotonic increasing function of  $T$ . In terms of these definitions, eq 11 becomes

$$K_{1T} = k_{10} \exp(h_1 t) + k_{20} \exp(h_2 t) \quad (14)$$

Using these notational simplifications, we were then able to mathematically prove<sup>25</sup> that it is possible, in principle, to determine all of the Gibbs free energy thermodynamic parameters, including in particular the two microconstants, for the two cationic microreactions of Figure 1 ( $k_1 = k_{10}$  and  $k_2 = k_{20}$  at the designated base temperature) by measurement of the cationic macroconstant at four different temperatures,  $K_{10}$ ,  $K_{11}$ ,  $K_{12}$ , and  $K_{13}$ . Thus, four parameters are necessary and sufficient when fitting the cationic macroconstants alone.

In order to simultaneously incorporate the anionic reaction path in the analysis, we merely note that if we include measurement of the anionic macroconstant,  $K_2$ , at the base temperature ( $K_{20}$ ), simple rearrangements of eq 3 yield both  $k_{12}$  and  $k_{21}$  at the base temperature ( $k_{120}$  and  $k_{210}$ ) as functions of the previously utilized macroconstants, i.e.,

$$k_{120} = \frac{K_{10}}{k_{10}} K_{20} \quad k_{210} = \frac{K_{10}}{k_{20}} K_{20} \quad (15)$$

Accordingly, we have determined the necessity for addition of one single further parameter.

Finally, to determine the parameterization required for characterizing the temperature variance of the anionic microreactions, we measure the anionic macroconstant at temperature  $T$ , i.e.,  $K_{21}$ , and note that, analogous to eq 15 we have

$$k_{12T} = \frac{K_{11}}{k_{1T}} K_{21} \quad k_{21T} = \frac{K_{11}}{k_{2T}} K_{21} \quad (16)$$

and where  $k_{1T} = k_{10} \exp(h_1 t)$  and  $k_{2T} = k_{20} \exp(h_2 t)$ . Therefore, for complete thermodynamic characterization of all microreactions for the two macroscopic deprotonation reactions of Figure 1, we require six and only six parameters. Accordingly, of the eight parameters produced from a naive expansion of the four sequence-specific deprotonation microreactions of Figure 1, i.e.,  $k_1$ ,  $h_1$ ,  $k_2$ ,  $h_2$ ,  $k_{12}$ ,  $h_{12}$ ,  $k_{21}$ , and  $h_{21}$ , two are superfluous. Consequently, we may readily eliminate one of the four microconstants and one of the four reduced enthalpies.

(25) See Supplementary Information.

To eliminate one of the four microconstant parameters, we introduce temperature-specific values of the zwitterion constant, i.e., analogous to eq 4, we have

$$\frac{k_{10}}{k_{20}} = k_{zw0} = \frac{k_{210}}{k_{120}} \quad (17)$$

Accordingly, we may use the quotient  $k_{10}/k_{20}$  in place of  $k_{20}$  and the product  $k_{120}k_{zw0}$  in place of  $k_{210}$ .

In order to eliminate one of the microenthalpy terms, we define the parameter  $\eta$ , such that

$$h_{21} = h_1 + \eta \quad (18)$$

i.e., we must in general allow for perturbation of the enthalpy change of a given microscopic deprotonation, e.g., 3-hydroxypyridinium to 3-hydroxypyridine, due to the protonation state of the tautomericly coupled site, i.e., 3-hydroxylate–pyridinium to 3-hydroxylate–pyridine. Using the Gibbs–Helmholtz expansion of eq 4, with eqs 17 and 18, we have

$$\frac{k_{10} \exp(h_1 t)}{k_{10}/k_{zw} \exp(h_2 t)} = \frac{k_{120} k_{zw} \exp[(h_1 + \eta) t]}{k_{120} \exp(h_{12} t)} \quad (19)$$

which after simplification and rearrangement leads to

$$h_{12} = h_2 + \eta \quad (20)$$

which forces us to conclude that said enthalpic perturbation is identical for both pairs of the tautomeric couple.

Accordingly, the final set of four Gibbs–Helmholtz microre-action equations in six parameters reads

$$\begin{aligned} k_{1t} &= k_{10} \exp(h_1 t) \\ k_{2t} &= k_{10}/k_{zw0} \exp(h_2 t) \\ k_{12t} &= k_{120} \exp[(h_2 + \eta) t] \\ k_{21t} &= k_{120} k_{zw0} \exp[(h_1 + \eta) t] \end{aligned} \quad (21)$$

and the temperature-dependent macroconstant equations become

$$K_{1T} = k_{10} \exp(h_1 t) + (k_{10}/k_{zw0}) \exp(h_2 t) \quad (22)$$

and

$$K_{2t}^{-1} = (k_{120} \exp[(h_1 + \eta) t])^{-1} + (k_{120} k_{zw0} \exp[(h_2 + \eta) t])^{-1} \quad (23)$$

for the cationic and anionic macroconstants, respectively. Finally, the tautomeric equilibrium is

$$k_{zw} = k_{zw0} \exp[(h_1 - h_2) t] \quad (24)$$

**Spectroscopic Determination of Enthalpies.** As will be demonstrated later, it will often be necessary to use absorption spectroscopy to determine the reduced microenthalpy terms  $h_1$

and  $h_2$ . We will now show the possibility of making these determinations.

If we choose to vary temperature and make (constant pH) spectral measurements at  $\tau$  different temperatures we have (analogous to eq 6)

$$\mathbf{A}_{w\tau} = \mathbf{E}_{w3} \mathbf{C}_{s\tau} \quad (25)$$

where  $\tau$  takes the place of  $p$ . It is of course possible to determine the total (sum) concentration of the isocoulombic pair, as well as the concentrations of the ionic species, via titration at constant temperature.<sup>26</sup> One may therefore readily determine the molar absorptivity coefficient spectra for the ions separately, i.e., the column vectors  $\mathbf{E}_{w1}$  and  $\mathbf{E}_{w4}$ , as well as that for the sum of the isocoulombic pair. We reiterate that the isocoulombic pair may not be resolved, one from the other since they are linearly dependent.

Consequently, we may with no loss of generality restrict our attention to the isocoulombic pair spectrum,  $\mathbf{O}_{w\tau}$ , where

$$\mathbf{O}_{w\tau} = \mathbf{A}_{w\tau} - \mathbf{E}_{w1} \mathbf{C}_{1\tau} - \mathbf{E}_{w4} \mathbf{C}_{4\tau} = \mathbf{E}_{w\xi} \mathbf{C}_{\xi\tau} \quad (26)$$

and where  $\xi = 2, 3$ , i.e.,  $\mathbf{O}_{w\tau}$  is the product of the isocoulombic submatrices of  $\mathbf{E}_{w3}$  and  $\mathbf{C}_{s\tau}$  in eq 25. Now for any given wavelength  $\lambda$ , and temperature  $t$ , we have

$$O_{\lambda t} = e_{\lambda 2} \frac{c_a k_{10} \exp(h_1 t) H_{\tau}}{D(H_{\tau}, t)} + e_{\lambda 3} \frac{c_a k_{20} \exp(h_2 t) H_{\tau}}{D(H_{\tau}, t)} \quad (27)$$

where it should be noted that  $D(H_{\tau}, t)$ , consisting as it does (cf. eq 9) solely of macroconstants and  $H_{\tau}$ , can be experimentally determined by means of potentiometric titrimetry. In order to use singular value decomposition (SVD) modeling (vide supra), one must separate out all components that are not explicit functions of temperature. As one may readily ascertain from eq 27, it is possible to do so by factoring out all multiplicative constant terms into one expression separate from the exponential microenthalpy functions. If we take

$$O_{\lambda t} = \left( \frac{e_{\lambda 2} c_a k_{10} H_{\tau}}{D(H_{\tau}, t)} \right) \exp(h_1 t) + \left( \frac{e_{\lambda 3} c_a k_{20} H_{\tau}}{D(H_{\tau}, t)} \right) \exp(h_2 t) \quad (28)$$

then the denominator function,  $D(H_{\tau}, t)$ , above must be measured or otherwise estimated a priori and then be properly incorporated into either the isocoulombic matrix or the microenthalpy matrix. We may then take each column vector of  $\mathbf{O}_{w\tau}$ , i.e., the absorbance spectrum at each temperature, and multiply it by the denominator function,  $D(H_{\tau}, t) \approx K_1 H_{\tau}$ , operative at that temperature to construct the "denominator-corrected" isocoulombic matrix  $\mathbf{S}_{w\tau}$ :

$$\mathbf{S}_{\lambda t} = (e_{\lambda 2} c_a k_{10}) \exp(h_1 t) + (e_{\lambda 3} c_a k_{20}) \exp(h_2 t) \quad (29)$$

or in matrix terms,

$$\mathbf{S}_{w\tau} = \mathbf{M}_{w\xi} \mathbf{X}_{\xi\tau} \quad (30)$$

(26) Kubista, M.; Sjoback, R.; Albinsson, B. *Anal. Chem.* **1993**, *65*, 994–8.

where the  $\mathbf{M}$  matrix consists of the terms (constants) in parentheses in eq 29 and  $\mathbf{C}$  consists of the exponential microenthalpy terms.

Equation 29 reveals that molar absorptivity coefficients and microconstants always occur together as products in the elements of matrix  $\mathbf{M}$  and hence may not be partitioned. Nonetheless it is apparent that, given measurements of  $D(H_{\tau}, t)$  for all temperatures of  $\mathbf{S}_{w\tau}$ , one may determine microenthalpies via nonlinear regression modeling using spectroscopy. Although one may model the system of eq 30 directly, there are various advantages to using multivariate methods, and we have chosen to use SVD modeling, as exemplified by Hug and Sulzberger.<sup>27</sup>

## EXPERIMENTAL SECTION

Titration were performed using an Orion expandable ion analyzer EA920 equipped with automatic temperature compensation and a digital thermometer. Titrations were performed with a  $\text{N}_2$  purge and temperatures were controlled to within 0.1 °C. The pH electrode, thermometer, and purge line were all inserted through a large rubber stopper which sealed a 100 mL beaker. Titrant was delivered with a (200–1000  $\mu\text{L}$ ) Finn pipette by removing a small rubber stopper from the main beaker stopper and quickly inserting/removing the pipet. 3-Hydroxypyridine was acquired from Aldrich and used as received. The pH electrode was calibrated prior to each titration using Fisher pH 4 and 10 buffers to two decimal digits, e.g., 10.00. The pH measurements, however, were recorded to three decimal digits (10.000). Two titrations, cationic and anionic, were performed at each temperature using 10 mM solutions, excluding 60 °C, where the cationic titration was not performed due to equipment failure.

The self-dissociation constant of water,  $K_w$ , was fit to a Gibbs–Helmholtz expression, assuming a linear change in enthalpy, over the temperature range 0–60 °C (cf. Albert and Serjeant,<sup>3</sup> Appendix II). The dielectric constant of water from 25 to 200 °C<sup>28</sup> was modeled with a simple exponential decay function using data at 10 MP and was then corrected to atmospheric pressure. This value was used to compute the (temperature-dependent) Debye–Huckel limiting law coefficient<sup>29</sup>  $A$  ( $A = 0.509$  at 25 °C) at the various temperatures.

Equilibrium constants were calculated using a full elaboration of the proton condition and were corrected for activity using the extended Debye–Huckel limiting law: assuming zero contribution to ionic strength from the zwitterion. Ion size parameters were taken from Kielland<sup>30</sup> with that for 3-hydroxypyridine assumed equal to 6.0.

UV spectroscopy was used to obtain macroconstants at room temperature, i.e., there was no thermostating of the sample cells. Solutions were 100  $\mu\text{M}$  in 3-hydroxypyridine and were pH buffered and prepared at a constant ionic strength of 0.01 M. Solutions were run in pseudorandom order. A thermostating fixture was acquired later and used to control cell temperature to within 0.1 °C using circulated water from a constant-temperature water bath. UV cell temperature was measured with a hand-held digital (thermocouple) thermometer. Thermostated solutions were not buffered but were simply 100  $\mu\text{M}$  in 3-hydroxypyridine.

(27) Hug, S. J.; Sulzberger, B. *Langmuir* **1994**, *10*, 3587–97, and references cited therein.

(28) *CRC Handbook of Chemistry and Physics*, 63rd ed.; CRC Press, Inc.: Boca Raton, FL, 1982; Table E-57.

(29) Castellan, G. W. *Physical Chemistry*, 2nd ed.; Addison-Wesley Publishing Co.: Reading, MA, 1971; Chapter 16.

(30) Kielland, J. *J. Am. Chem. Soc.* **1937**, *59*, 1675–8.

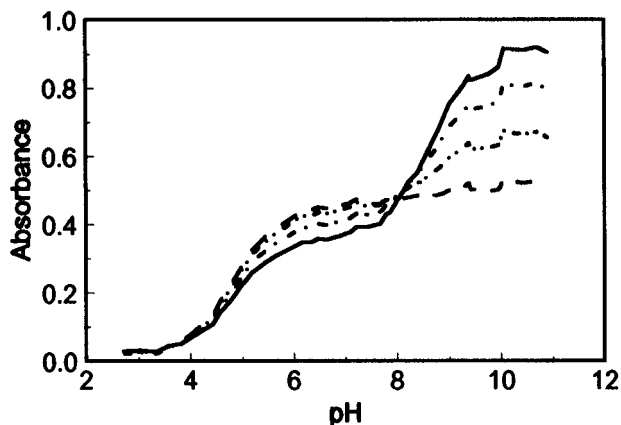


Figure 2. UV absorbance intensities for 100  $\mu$ M 3-hydroxypyridine as a function of pH for four specific wavelengths: 240 (solid), 242 (dash-dot), 244 (dash-dot-dot), and 246 (dash) nm.

Computations were performed on a Dell PC equipped with a 120-MHz pentium processor. Singular value decompositions with concomitant nonlinear regression were performed using MATLAB to procure macroconstants and enthalpies using UV data. Non-linear regression was performed on titration data to procure microconstant parameters using the Solver algorithm of Excel 4.0. The optimization dependent variable utilized was the simultaneous variation coefficient, CV, computed from both macroconstants together, i.e.,

$$CV = \sqrt{\sum_{i=1}^n \left( \frac{Kc_i - Kx_i}{Kx_i} \right)^2}$$

where  $Kc$  is the computed value for either macroconstant,  $Kx$  is the corresponding experimental value, and the index  $i$  runs over all temperatures for both macroconstants:  $K_1$  and  $K_2$ . Symbolic algebra was performed using Mathcad 5.0.

## RESULTS AND DISCUSSION

We initially set out to duplicate the procedure of Benesch and Benesch<sup>14</sup> (and others), who used the assumption of spectral invariance to coupled site protonation state. Figure 2 provides a visual indication of the approximate nature of this assumption in the case of 3-hydroxypyridine. What one hopes to find (experimentally) is a frequency region in the spectrum where change in pH produces little or no peak shift. By this we mean that the various moments describing a given peak, mode, mean, variance, skew, etc., are invariant to change in pH and that the only change is a monotonic (increasing or decreasing) variation in intensity. Such behavior would provide some degree of confidence for supposing spectral invariance. In fact, without exception, each UV peak of 3-hydroxypyridine undergoes a pronounced shift in frequency with change in pH. Therefore, without further corroborating evidence, the only conclusion one can reliably infer from Figure 2 is that there are two distinct macroscopic deprotonation steps. Figure 2 also provides an indication of the degree of subjectivity involved in assignment of microconstants by means of this procedure. Where the assumption of spectral invariance is accurate, the zwitterionic ratio,  $k_{zw}$ , is proportional to the ratio of the magnitudes of the two sigmoidal transitions occurring in each of the four isofrequency curves. Thus, the range of potential values for  $k_{zw}$  using this conjecture is quite large.

The data collected during this phase of the experiment was subjected to SVD with subsequent nonlinear regression modeling in order to determine the macroconstants, an estimate for the number of species, and the ion species spectra. Activity coefficient corrections were neglected here. The SVD algorithm decomposes an arbitrary data matrix,  $\mathbf{A}$ , into three matrices,  $\mathbf{A} = \mathbf{USV}^T$ , such that the fraction of the total variance in  $\mathbf{A}$ , which is accounted for by the orthogonal columnar basis vectors in  $\mathbf{U}$ , is provided by the square of the diagonal elements of  $\mathbf{S}$ .<sup>27</sup> The first four variance coefficients obtained by this procedure for our isothermal spectral data matrix,  $\mathbf{A}_{wp}$ , were as follows: 0.8774, 0.0744, 0.0478, and 0.0004. Hence, the last (fourth) term accounts for a full 2 orders of magnitude less variance than the third term, and from this we may conclude that, as expected, there are only three linearly independent species observable using isothermal spectra. The macro- $pK_a$ 's obtained in this fashion were 4.871 and 8.681, in good agreement with the titrimetric values despite the 100-fold difference in analyte concentration.

Having proven the theoretical possibility of establishing microconstants and associated site-specific thermodynamic parameters via temperature-variant (potentiometric) titrations, we then attempted to do so experimentally. What was observed was a fairly wide variation in estimated site-specific thermodynamic parameters and intersection temperatures. For example, we took the full, i.e., cationic and anionic, set of experimental data and performed the five-parameter nonlinear regressions resulting from having first specified the microconstant ratio parameter:  $k_{zw0}$ , for various values of  $k_{zw0}$ . As  $k_{zw0}$  varies from 1.00, representing microconstant pair equality, to 54.6,  $\exp(4)$ , the variance coefficient only varies from 0.0090 to 0.0087, a statistically negligible decrease of only 3%. This indicates that there is (experimentally) an excess of at least one degree of freedom in parameterization. Hence, accuracy would require that we measure at least one, and possibly more, of the six parameters by means of a method independent of titrimetry. This we were able to do via spectroscopic determination of the two site-specific microenthalpies.

As shown above, it is possible to determine the microenthalpy terms via measurement of the isocoulombic pair spectra across a range of temperature. We first made spectroscopic measurements at temperatures close to those measured titrimetrically. Next we used the full six-parameter optimized equation set (eq 22) to compute appropriately interpolated values of the  $K_{1t}$  macroconstants at the temperatures achieved for spectroscopic measurement. We then multiplied the spectrum at each temperature by the appropriate  $K_{1t}$  macroconstant (eq 29) to obtain the denominator-corrected isocoulombic matrix,  $\mathbf{S}_{wr}$ . Figure 3A shows four row vectors from the isocoulombic pair matrix,  $\mathbf{O}_{wt}$ , for the wavelengths representing the four peak maxima observed in the isocoulombic pair spectra. Note that three of the peaks decrease with increasing temperature, while one, 276 nm, increases with temperature. Since the row vectors are the weighted sums of the isocoulombic species concentrations (cf. eqs 26 and 27), Figure 3A provides a qualitative indication that there are at least two species extant in these spectra. Figure 3B demonstrates the corresponding row vectors from  $\mathbf{S}_{wr}$ . Finally, we used SVD nonlinear regression modeling on  $\mathbf{S}_{wr}$  to validate the hypothetical number (two) of species and then also to procure the two site-specific reduced microenthalpies,  $h_1$  and  $h_2$ . The first three basis spectra variance terms derived from  $\mathbf{S}_{wr}$ , vide infra, were 0.9954, 0.0040, and 0.0005. The microenthalpy values,  $\Delta H_1$  and  $\Delta H_2$ ,

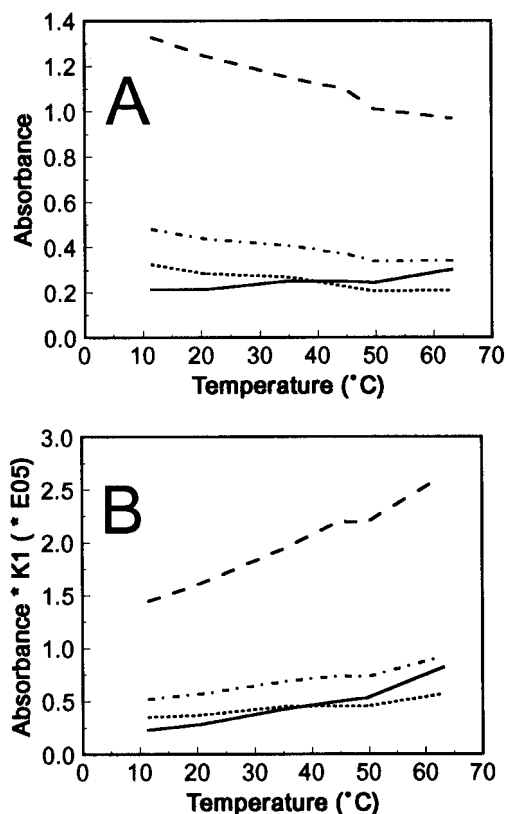


Figure 3. UV absorbance intensities for 100  $\mu\text{M}$  3-hydroxypyridine as a function of temperature for four specific wavelengths: 210 (dash-dot), 246 (dash-dot), 276 (solid), and 314 nm (dot). (A) Original (unmodified) absorbance intensities. (B) Product of absorbance intensities with the cationic macroconstant  $K_1$ , extant at the corresponding temperature.

Table 1. Optimized Microreaction Parameters for 3-Hydroxypyridine at 20  $^{\circ}\text{C}$

parameter	value $\pm$ std dev
$h_1$ (K)	$944 \pm 281$
$k_1$	$(1.164 \pm 0.061) \times 10^{-5}$
$h_2$ (K)	$5250 \pm 1210$
$k_{zw}$	$9.8 \pm 3.2$
$k_{12}$	$(1.751 \pm 0.003) \times 10^{-9}$
$\eta$ (K)	$-3315 \pm 8$

measured by this procedure were 1.88 and 10.4 kcal mol $^{-1}$  (7.87 and 43.5 kJ mol $^{-1}$ ), respectively.

Having procured reliable estimates for two of the six parameters, we next inserted these microenthalpy values as constants into the two macroconstant expressions (eqs 22 and 23) and then proceeded to optimize the remaining four parameters,  $k_{10}$ ,  $k_{zw}$ ,  $k_{12}$ , and  $h$ , using, as before, nonlinear regression on the titrimetrically measured macroconstants. In marked contrast to the previous five-parameter case, CVs for the three-parameter optimization resulting from having utilized the microenthalpy values measured above, with various values of the zwitterion ratio parameter,  $k_{zw}$ , considered as an independent variable, clearly relax to a reliable minimum (Figure S1, Supporting Information). The final values (using a base temperature of 20  $^{\circ}\text{C}$ ) for all six parameters are given in Table 1, and the temperature dependence of the various equilibria are graphically portrayed in Figure 4. The variance coefficient was 4.7% for  $K_1$  and was 3.0% for  $K_2$ .

By examining the difference between the calculated values for the macroconstants (closed diamonds, stars) and the quantitatively

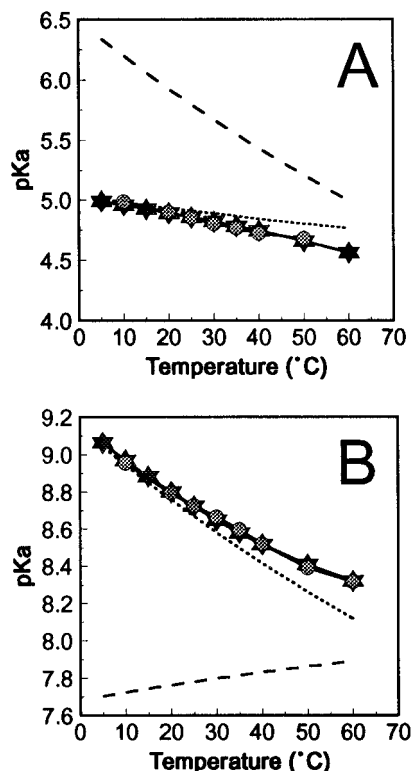


Figure 4. Experimental and computed macro- $pK_a$ 's, and computed micro- $pK_a$ 's for 3-hydroxypyridine as a function of temperature. (A) Cationic: circles, experimental values for  $pK_1$ ; stars, calculated values for  $pK_1$ ; dotted, calculated values for  $pK_1$ ; dashed, calculated values for  $pK_2$ . (B) Anionic: circles, experimental values for  $pK_2$ ; stars, calculated values for  $pK_2$ ; dotted, calculated values for  $pK_{12}$ ; dashed, calculated values for  $pK_{21}$ . Cationic calculations are via eq 22, and anionic calculations are via eq 23.

predominant microconstants (dotted lines) for both the cationic (Figure 4A) and anionic (Figure 4B) deprotonations, Figure 4 gives a visual indication of the error to be made by using the technique of Nygren et al.<sup>1</sup> for this particular case of 3-hydroxypyridine. Even at 5  $^{\circ}\text{C}$ , such error is readily discernible. Particularly given our interest in measurement of zwitterionic compounds whose  $k_{zw}$  is close to unity at room temperature, it may well often be the case that such error could be considerably more pronounced. Be that as it may, we contend that the procedure described herein is both more general and more accurate.

**Qualitative Identification.** Accurate measurement of the microconstants allowed us to compute the concentration of both isocoulomers as a function of temperature. This in turn allowed us to determine the molar absorptivity spectra for both isocoulomers, which we show in Figure 5B. The cation and anion spectra are included in Figure 5A and C, respectively. An internal comparison of all four species-specific spectra and analysis of related reference spectra are consistent with assigning the spectrum of species 2 to that of the zwitterion and the spectrum of species 3 to that of the neutral isocoulomer.<sup>25</sup> We assert that the extracted spectra are so readily rationalized that they corroborate the efficacy of our technique. Hence, we substantiate the deduction of Metzler and Snell,<sup>31</sup> that the zwitterion predominates at room temperature. One notes from examination of these spectra that in the region of 240 nm, and again in the region of

(31) Metzler, D. E.; Snell, E. E. *J. Am. Chem. Soc.* **1955**, *77*, 2431–7.

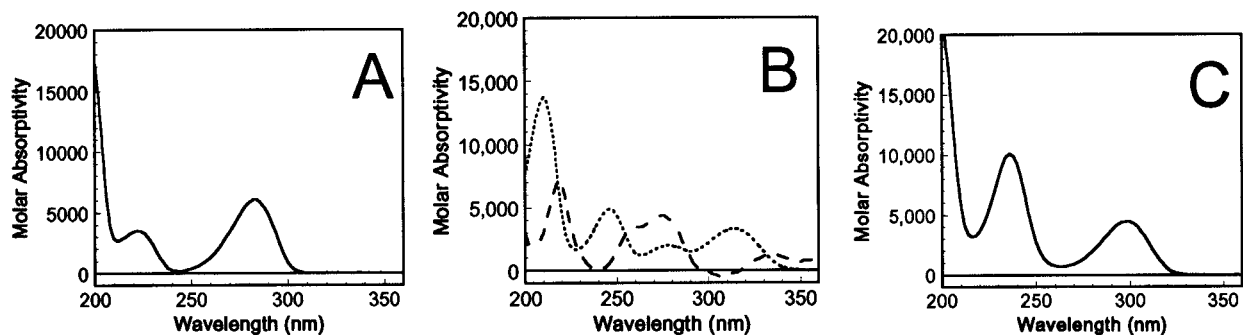


Figure 5. Molar absorptivity spectra of 3-hydroxypyridine. (A) Cation. (B) The two isocoulombic species, zwitterion (dotted) and unpolarized neutral (dashed). (C) Anion.

Table 2. Thermodynamic Microreaction Parameters ( $\text{J mol}^{-1}$ ) for 3-Hydroxypyridine at  $25\text{ }^\circ\text{C}^a$

	1	2	12	21
$k$	$1.23 \pm 0.06 (0.17) \times 10^{-5}$	$1.2 \pm 0.2 (0.5) \times 10^{-6}$	$2.15 \pm 0.05 (0.10) \times 10^{-9}$	$2.1 \pm 0.4 (0.9) \times 10^{-8}$
$\Delta G$	$28\ 000 \pm 130 (330)$	$33\ 100 \pm 610 (1560)$	$49\ 476 \pm 4 (9)$	$44\ 400 \pm 800 (2100)$
$\Delta H$	$7800 \pm 2300 (4000)$	$44\ 000 \pm 10000 (22\ 000)$	$30\ 000 \pm 10000 (25\ 000)$	$-6000 \pm 200 (5700)$
$\Delta S$	$-68.8 \pm 7.9 (20.2)$	$36 \pm 34 (87)$	$-66 \pm 34 (83)$	$-169 \pm 8 (21)$

<sup>a</sup> Uncertainties are standard deviations and (0.95 confidence interval). Each column represents a different microreaction sequence.

310 nm, that the only responsive spectrum is that of the zwitterion. Close examination of these peaks indicates that any temperature variance of the zwitterion spectrum is relatively minor and thus provides additional confidence, post hoc, in the reliability of the microenthalpy values as determined by SVD nonlinear regression modeling. Moreover, examination of Figure 5 emphatically illustrates the difficulty in selecting, a priori, a frequency region where moiety spectral invariance holds true.

**Regression Statistics.** In order to produce statistical inferences about the (nonlinear regression) parameter set, we estimated the approximate variance–covariance matrix:  $\mathbf{s}^2(\mathbf{D})$ , of the regression coefficients as<sup>32</sup>

$$\mathbf{s}^2(\mathbf{D}) = \text{MSE}(\mathbf{D}\mathbf{D})^{-1} \quad (31)$$

where  $\mathbf{D}$  is the matrix of partial derivatives, i.e., the Jacobian, of the temperature-dependent macroconstant ( $K_{1t}$ ) with respect to the microconstants parameters, i.e.,

$$\frac{\partial K_{1t}}{\partial k_{10}}, \frac{\partial K_{1t}}{\partial k_{20}}, \frac{\partial K_{1t}}{\partial h_1}, \frac{\partial K_{1t}}{\partial h_2}, \frac{\partial K_{1t}}{\partial k_{120}}, \frac{\partial K_{1t}}{\partial \eta}$$

evaluated for each temperature of  $\mathbf{S}_{wr}$  at the final nonlinear regression estimate of those parameters. Using the five (inclusive) wavelengths between 210 and 218 nm, i.e., 22 degrees of freedom, we estimate the 95% confidence interval (CI) for the microenthalpies as 960 (4050 J) and 5200 cal (21800 J), respectively. These SEM values correspond to 0.95 CI variation coefficients of 0.51 and 0.50; hence, we have eliminated the possibility of nonsingular codependence of the two microenthalpies.

We then obtained the variance-covariance matrix for the pair of parameters  $k_{10}$  and  $k_{20}$ , using macroconstant  $K_{1t}$  data only. Variability in the microenthalpy parameters  $\Delta H_1$  and  $\Delta H_2$  was not

Table 3. Comparison of Experimental and (SPARC) Computed  $\text{p}K_a$ 's at  $25\text{ }^\circ\text{C}$

	experimental <sup>a</sup>	SPARC
$\text{p}k_1$	4.91	5.0
$\text{p}k_2$	5.90	5.8
$\text{p}k_{12}$	8.668	8.5
$\text{p}k_{21}$	7.67	7.7

<sup>a</sup> Significant digits only.

factored into these computations. The variance–covariance matrix for the pair of parameters  $k_{120}$  and  $h$  was obtained using macroconstant  $K_{2t}$  data only, again without factoring in variability in the other four parameters. Microspecies thermodynamic parameters at  $25\text{ }^\circ\text{C}$  along with their variance estimates are given in Table 2. Measured values for the microconstants ( $25\text{ }^\circ\text{C}$ ) are compared to those computed by the SPARC algorithm in Table 3. Deviations of the SPARC computed microconstants from those measured here are well within previously established error estimates for the algorithm (vide infra).

## CONCLUSION

The only assumptions required of this method are quantitative and not qualitative in nature and contribute only to the extent of random, as opposed to systematic, error. These assumptions are, first, that both microenthalpies and species spectra are effectively constant throughout the temperature range under consideration. (We are currently investigating the prevalence and significance of the temperature-induced UV spectral shift phenomenon of Saliel et al.<sup>23</sup>), second, that the magnitudes of the two microenthalpies as well as the degree of resolution between the spectra of the two isocoulombers, are sufficient for the change in relative proportion of said isocoulombers to be discernible at several temperatures. This last is a reasonable assumption in the UV domain and is, given sufficient sensitivity, an excellent assumption using more qualitatively informative spectra, as are those of NMR or vibrational spectroscopy; and, finally, that one

(32) Neter, J.; Wasserman, W.; Kutner, M. H. *Applied Linear Statistical Models*, 2nd ed.; Richard D. Irwin, Inc.: Homewood, IL, 1985; Chapter 14.

may explicitly account for the presence of conformers when necessary.

Accordingly, we have hereby produced the first general self-checking method for accurate experimental measurement of tautomeric acidity equilibrium (micro)constants, the first resolved UV spectra of isocoulomers, species that are linearly codependent throughout any isothermal pH domain, and the first verification of a SPARC microconstant parameter set. While we here measured macroconstants by means of potentiometric titrimetry, it is in general more accurate to do so by means of spectroscopy.<sup>3</sup> When one includes the necessity, as here, to produce spectra as a function of temperature in order both to independently assess microenthalpies and to provide qualitative species identification, then information-rich spectroscopic measurement becomes relatively more efficient than titrimetry as well. Hence, due to its compatibility with aqueous samples, and given recent advances in the sensitivity of its instrumentation, viz., owing primarily to the exceptionally high quantum efficiencies of modern charge coupled device (CCD) detectors, and to the high spectrometer throughput which results from employing notch filters that efficiently remove Rayleigh scattering, Raman spectroscopy appears to be an optimum tool to apply in this arena. We are therefore in the process of constructing a refined and definitive microconstant measurement device, a notch-filtered, CCD-based, imaging Raman spectrometer that is fiber-optically coupled to an autotitration apparatus, for simultaneous automated measurement of all necessary observables.

#### ACKNOWLEDGMENT

This research was supported in part by an appointment (J.C.D.) to the Postgraduate Research Participation Program at the National Exposure Research Laboratory (Athens, GA) administered by the Oak Ridge Institute for Science and Education through an interagency agreement between the U.S. Department of Energy and the U.S. Environmental Protection Agency. The authors also thank Drs. Sam Karickhoff (EPA), Lionel Carreira (UGA), and Said Hilal (NRC) for their helpful and lively discussions. We also thank Mr. George D. Yager (EPA) for his various technical contributions. Note: Mention of trade names or commercial products does not constitute endorsement or recommendation for use by the U.S. Environmental Protection Agency.

#### SUPPORTING INFORMATION AVAILABLE

(1) A formal mathematical proof of our contention that the four microconstant parameters of eqs 11, 14, and 22, may be determined from four cationic macroconstants extant at four different specified temperatures; (2) interpretation and rationalization of the spectra of Figure 5; (3) Figure S1 demonstrating the statistical reliability of our procedure (8 pages). Ordering and access information is given on any current journal masthead page.

Received for review September 11, 1996. Accepted February 10, 1997.<sup>⊗</sup>

AC960922D

---

<sup>⊗</sup> Abstract published in *Advance ACS Abstracts*, March 15, 1997.